Hydrogeochemistry and cation-exchange processes in the coastal aquifer of Mar Del Plata, Argentina

D. E. Martínez · E. M. Bocanegra

Abstract The aquifer of Mar del Plata is unconfined and composed of silt and fine sand. The sand fraction is mainly quartz, potassium feldspars, chalcedony, and gypsum. Volcanic-glass shards (40–60%) dominate the silt fraction, and the clays are of the smectite and illite groups. Calcium carbonate, in caliche form, constitutes about 10–20% of the sediment.

Groundwater flow is from west to east, and discharge is in the Atlantic Ocean. Because of overexploitation, the flow direction was reversed in a coastal belt about 3.5 km wide, and this has resulted in seawater intrusion. The groundwater is the $CaHCO_3$ type in the recharge zone, and becomes $NaHCO_3$ type towards the discharge area. Salinization by marine intrusion and seawater/fresh-water mixing produces an increase in the major-ion concentrations of the groundwater. The calcium content of the groundwater is higher and the sodium content is lower than those that would be expected if the mixing is considered as just the addition of seawater and fresh water in determined proportions without reactive processes taking place.

Hydrogeochemical modeling was applied to the study of hydrogeochemical processes, mainly cation exchange, using the codes NETPATH and PHREEQM. Calcite and gypsum equilibrium, together with cation exchange, are the main hydrogeochemical processes. Cation-exchange capacity of the solid phase was determined by empirical calculations and experimental methods. The affinity order for the groundwater in contact with the aquifer matrix is Ca>Mg>Na in the regional-flow system, but the order is reversed in the salinization process. Reactive transport modeling using the code PHREEQM is useful for analyzing cation exchange in a marine-intrusion process.

Received: 26 March 1999 / Accepted: 1 March 2002
Published online: 24 April 2002

D.E. Martínez (✉)
Consejo Nacional de Investigaciones Científicas
y Técnicas (CONICET) – Centro de Geología de Costas
y Cuaternario. Universidad Nacional de Mar del Plata.
Casilla de Correo 722-(7600) Mar del Plata, Argentina
e-mail: demarti@mdp.edu.ar

E.M. Bocanegra
Comisión de Investigaciones Científicas de la Provincia
de Buenos Aires.-Centro de Geología de Costas y Cuaternario.
Universidad Nacional de Mar del Plata.
Casilla de Correo 722-(7600) Mar del Plata, Argentina

Résumé L'aquifère de Mar del Plata est libre et constitué de silt et de sable. La fraction sableuse contient principalement du quartz, des feldspaths potassiques, de la chalcédoine et du gypse. La fraction silteuse contient des fragments de verre volcanique (40–60%) et les argiles appartiennent aux groupes des smectites et des illites. 10–20% du sédiment sont du carbonate de calcium, sous forme d'un caliche.

L'écoulement de la nappe s'effectue de l'ouest vers l'est, pour se décharger dans l'Océan Atlantique. Du fait de la surexploitation, l'écoulement s'est inversé dans une bande littorale large d'environ 3,5 km, ce qui a produit une intrusion marine. Le faciès de l'eau souterraine est bicarbonaté calcique dans la zone de recharge et devient bicarbonaté sodique dans la zone de décharge. La salinisation par intrusion marine et par mélange eau douce/eau salée produit un accroissement des concentrations en ions majeurs de l'eau souterraine. La concentration en calcium de l'eau souterraine est plus élevée et celle en sodium est plus faible que ce que devrait donner un simple mélange d'eau de mer et d'eau douce en proportions bien définies, en l'absence de processus réactifs.

Une modélisation hydrogéochimique a été réalisée afin d'étudier les processus hydrogéochimiques, principalement des échanges de cations, au moyen des codes NETPATH et PHREEQM. Les équilibres de la calcite et du gypse sont, avec les échanges de cations, les principaux processus hydrogéochimiques. La capacité d'échange de cations de la phase solide a été déterminée par des calculs empiriques et des méthodes expérimentales. L'ordre d'affinité de l'eau souterraine au contact de la matrice de l'aquifère est Ca> Mg> Na, dans le système aquifère régional ; mais cet ordre est inversé dans le processus de salinisation. La modélisation du transport réactif au moyen du code PHREEQM est utile pour analyser l'échange de cations dans un processus d'intrusion marine.

Resumen El acuífero de Mar del Plata es un acuífero libre, formado por sedimentos limosos o arenosos finos.

 DOI 10.1007/s10040-002-0195-7

La fracción arena se compone de plagioclasas, cuarzo, feldespato potásico, calcedonia y yeso. En la fracción limo (40–60%) se destaca el predominio de trizas de vidrio volcánico, mientras que las arcillas son del tipo de las esmectitas e illita. El $CaCO_3$ constituye entre 10–20% del sedimento en forma de concreciones y costras.

El flujo subterráneo regional es de oeste a este, con descarga en el Océano Atlántico. Como consecuencia de la sobreexplotación, se produjo la intrusión de agua de mar en el acuífero, afectando una franja de 3,5 km de ancho.

Las aguas subterráneas son de composición $CaHCO_3$ en el área de recarga, haciéndose $NaHCO_3$ hacia las zonas de descarga. En el proceso de salinización por intrusión marina se produce un incremento general en la concentración de iones y una tendencia a aumentar la concentración de calcio y a disminuir la de sodio con respecto a la mezcla conservativa.

El estudio de los procesos hidrogeoquímicos se ha efectuado por medio de la modelación hidrogeoquímica utilizando los códigos NETPATH Y PHREEQM. El equilibrio con los minerales calcita y yeso y el intercambio de cationes han sido identificados como los principales procesos hidroquímicos. El intercambio de cationes fue particularmente analizado. La capacidad de intercambio catiónico de la fase sólida fue determinada por métodos empíricos y experimentales. La afinidad de los cationes por la matriz del acuífero presenta un orden Ca> Mg> Na en el caso del flujo regional. En el caso de la intrusión marina el orden de afinidad es inverso. La modelación con el código PHREEQM del transporte reactivo es útil para analizar el intecambio catiónico en procesos de intrusión marina.

Keywords Argentina · Cation exchange · Hydrochemical modeling · Salt-water/fresh-water relations

Introduction

Background

Cation exchange is one of the most important geochemical processes taking place in aquifers, but, as pointed out by Sposito (1984), it is sometimes difficult to distinguish between exchange and other reactions. This difficulty arises from poor knowledge of the exchange surfaces, the scarcity of values for exchange coefficients, and the difficulty in assigning activities to the sorbed cations.

Seawater intrusion into aquifers occurs in many areas of the world, including, for example, Barcelona, Spain (Custodio 1987), Sonora, Mexico (Steinich et al. 1998), California, USA (Banks et al. 1957), and the Biscayne aquifer, Florida, USA (Kohout 1960). Generally, intrusion results from overexploitation of aquifers. Two types of problems associated with overexploitation and marine intrusion are (1) those related to decline in potentiometric surfaces, and (2) those related to increased salinization of the groundwater.

One of the most dramatic cases of salinization occurred in Tripoli, Libya, where, in just 17 years the total dissolved-solids content of the groundwater increased from 265–675 mg/L in 1976 to 10,000 mg/L in 1993 (El-Baruni 1995).

Bocanegra and Custodio (1994), in a comparative study of the coastal aquifers of Barcelona, Spain, and of Mar del Plata, Argentina, showed that, in both areas, the overexploitation of the aquifers resulted in significant decline of the potentiometric surfaces, in increasing aquifer salinization, in wells being shut down, and problems related to water-level recovery. Since that time, water levels in Mar del Plata have recovered as much as 10 m, which has led to the flooding of cellars and underground structures and corrosion of metal structures. Similarly, in Barcelona underground car parks and subway tunnels have been flooded. In both aquifers, water quality has been seriously degraded as a consequence of changes in the hydraulic gradient. In both Mar del Plata and Barcelona, many wells have been shut down because of water salinization, at a substantial cost.

From a geochemical perspective, aquifer salinization consists of a high-salinity solution (seawater) mixing with a dilute solution (fresh water) in a medium that has many reactive solids, such as minerals. In coastal aquifers, where the relationship between seawater and fresh water is complex, cation exchange contributes significantly to the final composition of the groundwater. In salt-water/fresh-water mixing, the water and aquifer matrix reach a different equilibrium state, a nonlinear change in chemical properties takes place, there is redistribution of carbon-bearing species, and a nonlinear dependence of the activity coefficients on ionic strength (Wigley and Plummer 1976).

Fresh water in coastal areas is commonly dominated by HCO_3^- ions because the addition of the large amounts of CO_2 from the root zone, and calcite, if present, is dissolved (Back et al. 1979). In carbonate-rock aquifers, $CaCO_3$ dissolution is the most common process (Nadler et al. 1980; Bosch and Custodio 1993; Manzano et al. 1993). The reaction of different carbonate minerals in the mixing zone produces many characteristic phenomena, such as aragonite and calcite replacement or dolomitization, which modifies the hydrologic properties of the aquifer (Back and Herman 1991). Sulfate reduction is also a typical reaction in some salt-water/fresh-water mixing (Nadler et al. 1980; Bosch and Custodio 1993). The reaction involves organic-matter oxidation in a reducing anoxic environment:

$$2CH_2O + SO_4^{2-} \rightarrow 2HCO_3^- + H_2S \quad (1)$$

In detrital sedimentary aquifers, cation exchange is one of the most important geochemical processes of seawater intrusion. In a case study in Belgium, Walraevens et al. (1993) report that salinization starts with an increase in ion concentrations, which is quickly followed by cation exchange, in which Ca^{2+} is released and the marine cations Na^+, K^+, and Mg^{2+} are absorbed. Cation exchange is

 DOI 10.1007/s10040-002-0195-7

the most noticeable hydrogeochemical process in the movement of the saline front in the detrital aquifer of Oropesa, Spain (Giménez et al. 1995). The characteristic cation-exchange process that takes place when seawater intrudes a coastal fresh water aquifer is:

$$Na^{+} + {}^{1}/_{2}Ca{-}X_2 \rightarrow Na{-}X + {}^{1}/_{2}Ca^{2+} \quad (2)$$

where *X* indicates the exchanging solid surface.

During fresh-water or salt-water displacement in aquifers, the solute cations may become separated because of cation exchange, a phenomenon that is known as ion chromatography (Beekman 1991; Appelo 1993; Appelo and Postma 1993). In this process, because of the different selectivity of natural cation exchangers for different cations, solute cations become separated in space. Examples of the application of the ion-chromatography theory to field data are found in Manzano et al. (1993) and Stuyfzand (1993, 1999). Stuyfzand (1993, 1999) shows an interesting cross section of the coastal area of northwestern Netherlands that displays the distribution of hydrochemical facies resulting from salt-water intrusion.

The Mar del Plata Aquifer

The Mar del Plata aquifer in Argentina is an unconfined coastal aquifer in which seawater has intruded as much as 3.5 km inland. The seawater intrusion has been described by Groeber (1954) and Sala et al.(1980), but they make only a brief reference to cation exchange. A more complete analysis of the sea-water/fresh-water mixing by Bocanegra et al. (1993) evaluates the potentiometric and hydrochemical evolution of the area. Bocanegra (1993) and Martínez et al. (1995) further investigated geochemical aspects of marine intrusion in Mar del Plata by applying hydrogeochemical modeling. Using the earlier works of Bocanegra (1993), Martínez et al. (1995), and Martínez and Bocanegra (1998) as a basis, the aim of this paper is to contribute to a better understanding of the aquifer geochemistry and the salinization problem through a detailed study of the cation-exchange processes.

Hydrogeological Setting

Mar del Plata is the main Argentine seaside resort on the Atlantic coast. It has a population of about 600,000, which doubles in the summer. Groundwater is the only available water resource for drinking, agricultural, and industrial use. Mar del Plata, shown in Fig. 1, is located on the northeastern side of the Tandilia Range, also called the Sierras Septentrionales de la Provincia de Buenos Aires. The Tandilia Range, which has a maximum altitude of about 40 m above mean sea level in the Mar del Plata area, consists of quartzite of the lower Paleozoic Balcarce Formation (Dalla Salda and Iñiguez 1979), which is broken into horsts and grabens by three fault systems (Teruggi and Kilmurray 1980).

A sedimentary cover about 100 m thick, of unconsolidated upper Tertiary and Quaternary silt and silty sand,

Fig. 1 Location of the Mar del Plata area, Argentina

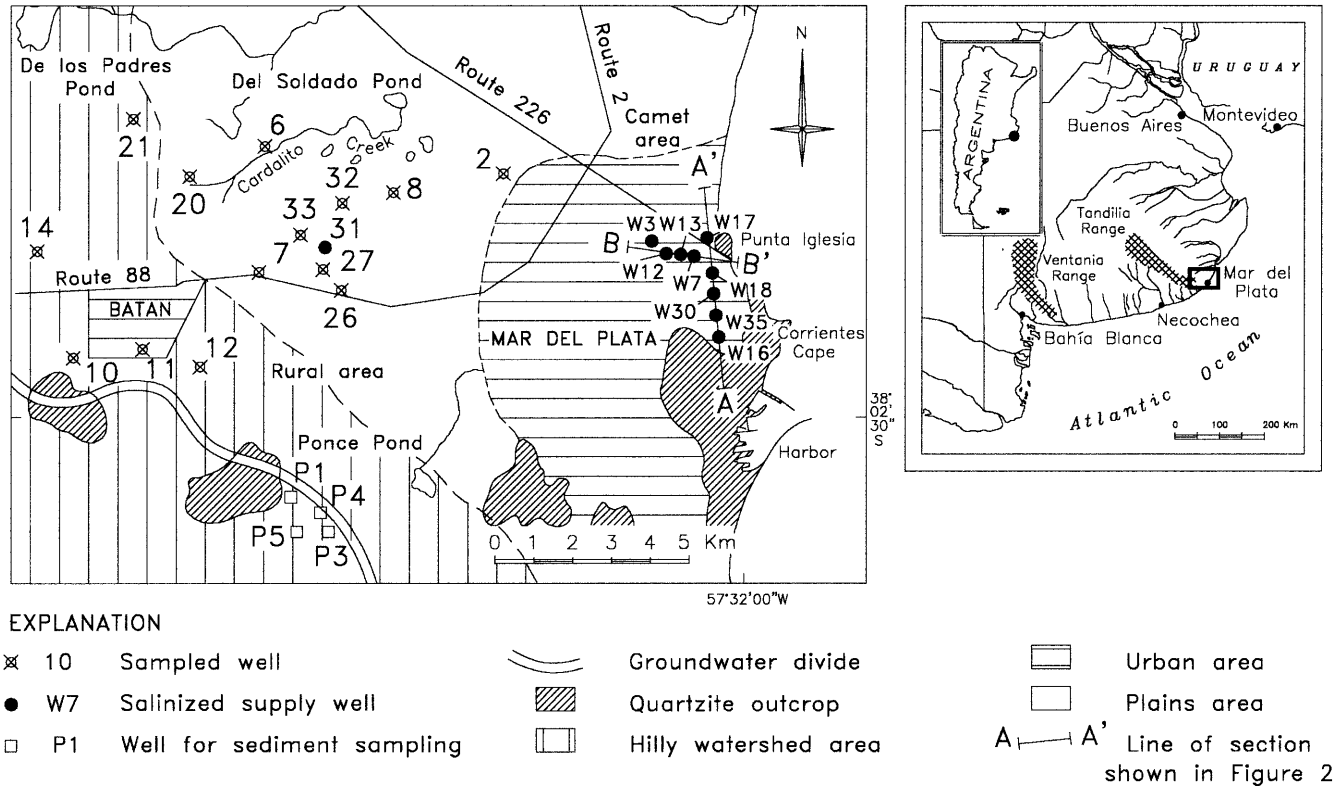

 DOI 10.1007/s10040-002-0195-7

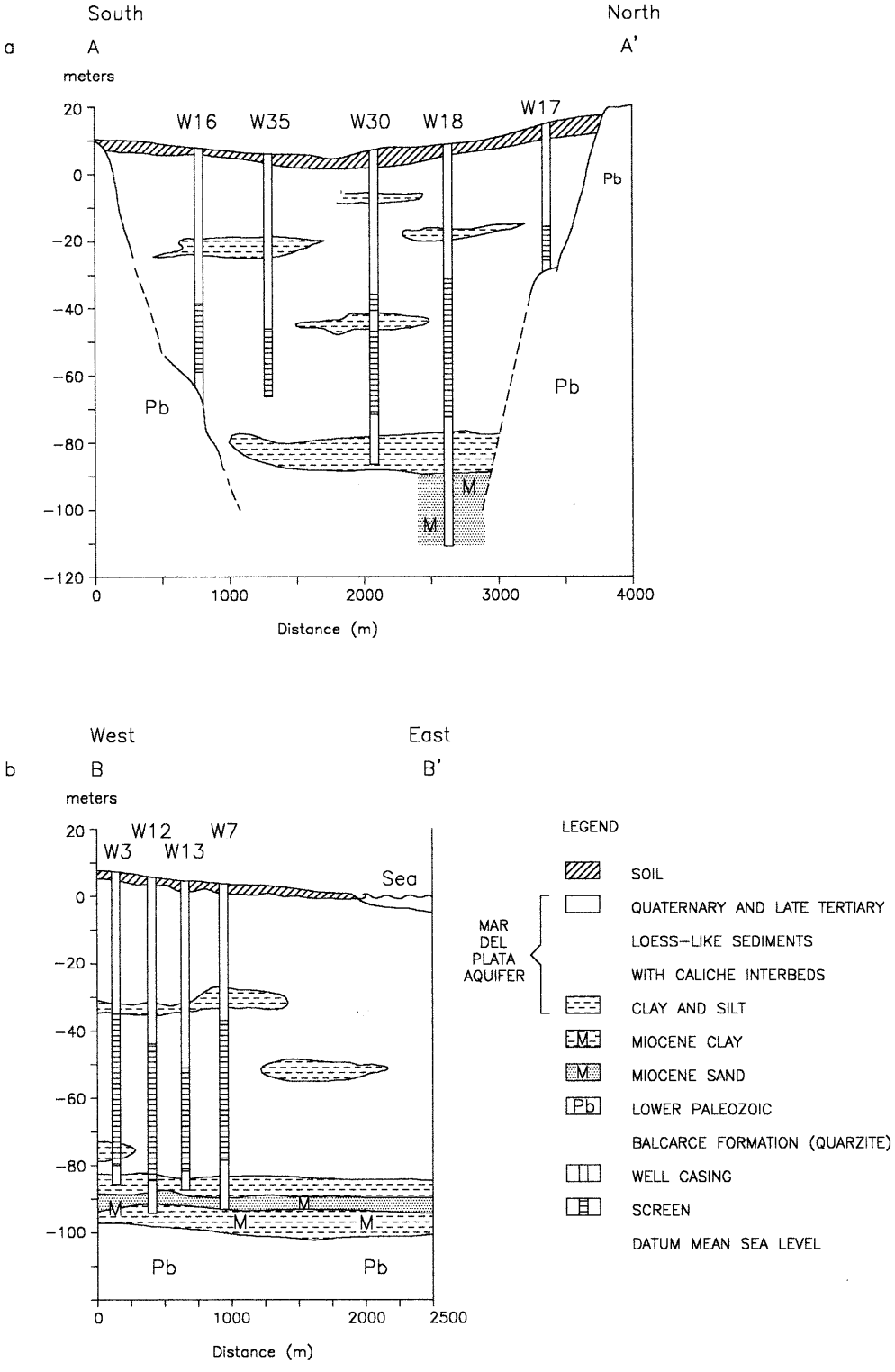

Fig. 2 Geological cross sections in Mar del Plata aquifer adjacent to the Atlantic Ocean. Location of wells and cross sections shown in Fig. 1

overlies quartz bedrock. Miocene clayey and sandy strata are present at a depth of 60 m in some parts of the grabens. The Quaternary deposits, called "Pampean sediments" or loess-like sediments, are the most important hydrogeological sequence, ranging in thickness from 70–100 m, as shown in Fig. 2, although similar physically to loess, these sediments are mostly reworked loess, having been transported and deposited by streams.

The "Pampean sediments" that crop out in the coastal cliffs of Mar del Plata, as described by Teruggi (1957), consist of a sand fraction (very fine to fine sand), mainly composed of plagioclase feldspars, which ranges from

 DOI 10.1007/s10040-002-0195-7

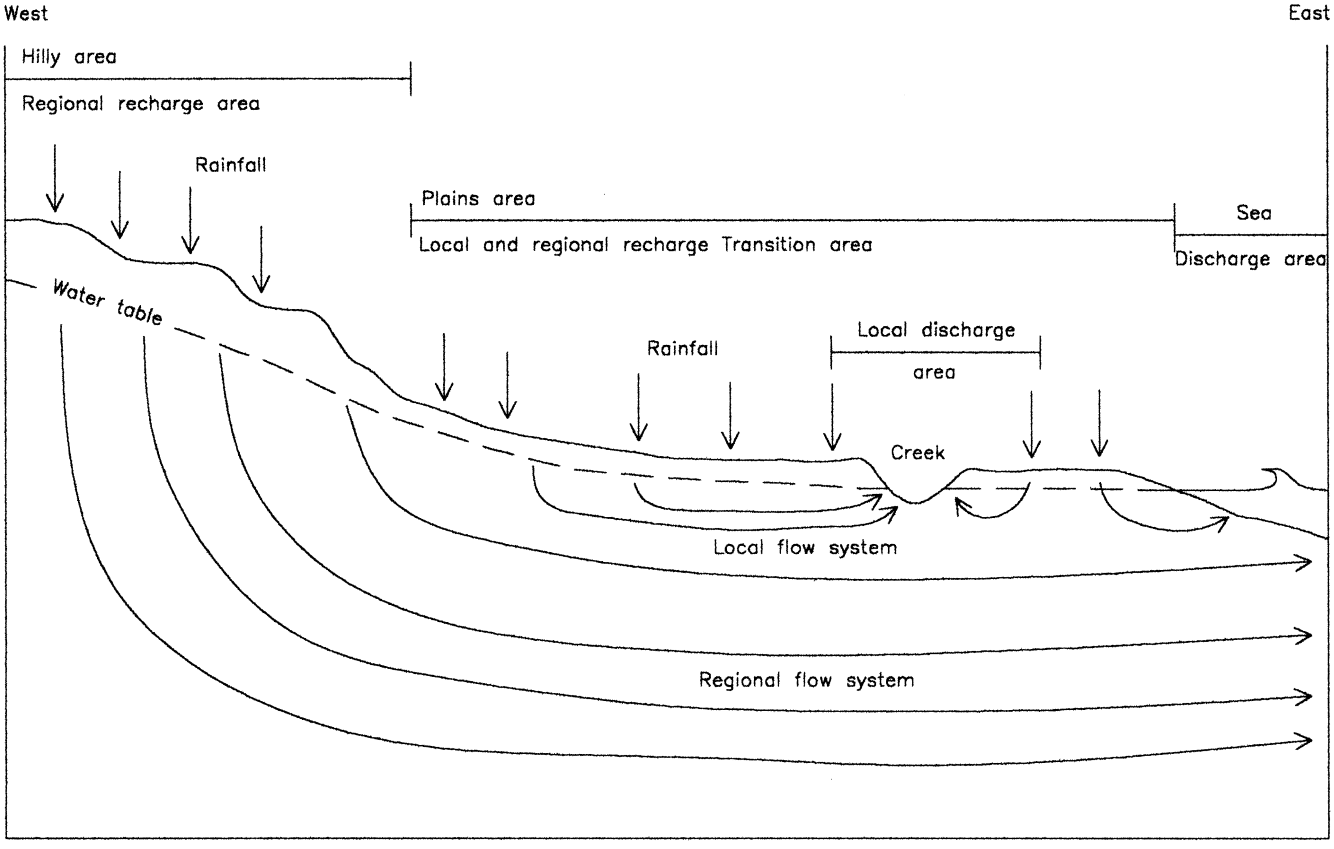

Fig. 3 Schematic section along the groundwater flow path, Mar del Plata aquifer

30–50% by weight. Labradorite is the most common type, followed by andesine and oligoclase. Quartz makes up less than 20% of the sand fraction, and volcanic glass is 1–25%. Orthoclase, chalcedony, gypsum, and fragments of argillaceous rocks are sparse. The silt fraction consists of volcanic glass shards (40–50%), plagioclase feldspar, quartz, and orthoclase. Gypsum, in fibrous crystals, is generally sparse, but in places is as much as 20%. The clay fraction is mainly montmorillonite.

The mineralogy, described by Martínez et al. (1998) from drilling samples, differs somewhat from that reported by Teruggi (1957), mainly in the types of clay. The clays are principally smectite and a subordinate amount of illite, increasing in crystallinity with depth. The fine-sand fraction constitutes the major portion of the sediment, consisting mainly of quartz, plagioclase feldspars, K-feldspars, muscovite, volcanic glass, oxides, calcite, dolomite, olivine, and amorphous silica, in decreasing order of abundance. Osterrieth (1992) reports the occurrence of iron sulfide in the sediments exposed in the coastal area, which probably formed during Pleistocene and Holocene marine advances.

Near the surface of Mar del Plata, the "Pampean sediments" form an unconfined aquifer with changes in permeability resulting from subtle changes in grain size and local increases of clay content. The clayey beds vary in thickness and are laterally discontinuous.

The transmissivity and storativity of the aquifer have been determined in 28 wells by means of pumping and single-well recovery tests during the development of each well by the water-supply organization (Obras Sanitarias). Because of variations in the aquifer thickness, the transmissivity is 600–800 m^2/day in urban areas and 1,000–1,400 m^2/day in rural areas (Fig. 1). The storativity, based on pumping tests, is 0.001. Estimated hydraulic conductivity is 10–15 m/day. Porosity measured by a volumetric procedure described in Custodio and Llamas (1976) ranges from 0.20–0.30.

The average rainfall from 1901–1987 in Mar del Plata was 851 mm/year. The warm season (October–March) is usually rainy and has two rainfall peaks (December and March); the cold season (April–September) is less rainy, and minimum rainfall occurs in July and August. According to Thornthwaite's method (Thornthwaite 1948), the potential evapotranspiration (ET) is 720 mm/year. The excess of ET over rainfall is 132 mm/year, which occurs between June and October. Recharge to the Mar del Plata aquifer system is from infiltration of rainfall throughout the area. Recharge to the regional groundwater flow system is from the hilly area along the water divide (Fig. 1); recharge to the local flow system is from the plains area near the coast. These relationships are shown in Fig. 3. The natural discharge is toward the sea, but surface streams are discharge areas for shallow groundwater (Fig. 3).

At the beginning of the twentieth century, groundwater flow was seaward, but over time intensive exploita-

 DOI 10.1007/s10040-002-0195-7

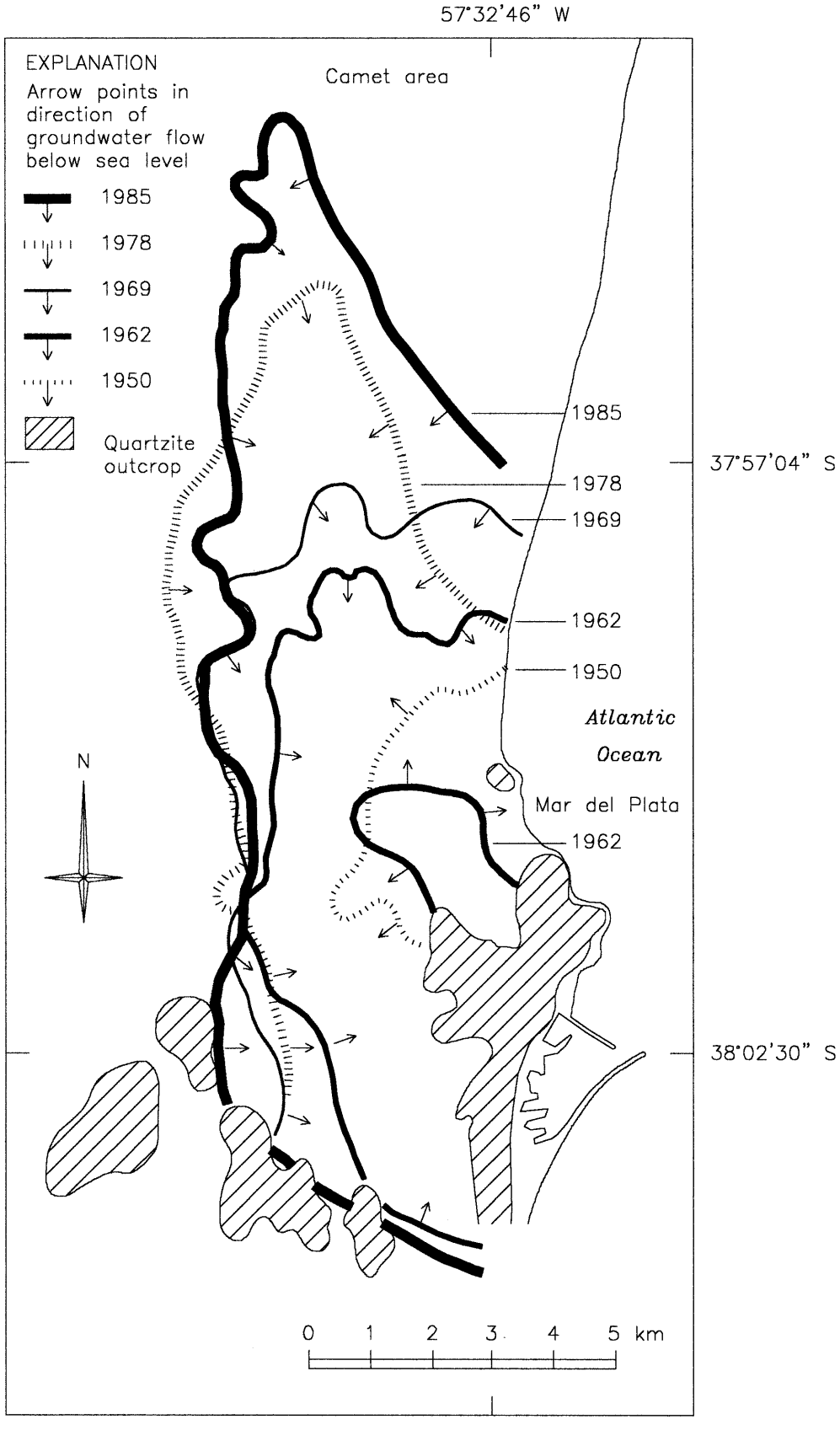

Fig. 4 Location of the zero potentiometric contour, Mar del Plata aquifer, in various years from 1950–1985

 DOI 10.1007/s10040-002-0195-7

tion of the groundwater has induced intrusion of salt water into the aquifer in a wide belt of the urban area and a significant decline in water level has occurred. By 1950, a large cone of depression in the water table had developed in the urban area; the cone extended over 15 km^2 and the maximum drawdown was 10 m. In 1955, a second cone of depression, covering 30 km^2, developed around the harbor. The situation became critical in 1969 when the cones of depression had expanded to 90 km^2, as depicted in Fig. 4, and the water table had declined as much as 23 m in urban areas. After 1969, pumping of wells in the Camet area (Fig. 1) caused the zero-altitude potentiometric contour on the water table to migrate northward rather than westward, to a position 7.5 km from the coast (Bocanegra et al. 1993).

The groundwater is a calcium-bicarbonate type in the hilly recharge area and a sodium-bicarbonate type in the transition and discharge areas. In areas unaffected by seawater intrusion, the solute concentration (TDS) increases by natural hydrochemical processes from 500 mg/L in the recharge area to 1,200 mg/L in the discharge areas.

Methodology

The sedimentary material of the Mar del Plata aquifer, which adsorbs constituents from the infiltrating water, was studied from samples of well cuttings. Grain-size determinations were performed using sieving and pipette techniques (Carber 1971); organic matter was determined by the method of Walkey and Black (1965); and clay mineralogy was identified by X-ray diffraction. The cation-exchange capacity (CEC) of the samples was determined by conventional techniques in the Soils Laboratory of the INTA (National Institute of Agricultural Technology, Argentina).

The data on the chemistry of groundwater from the salinized area, from Obras Sanitarias, the governmental organization for water supply, include more than 1,000 groundwater analyses from 1950 to the present. This database contains groundwater-quality data from about 60 wells in the urban area, which were in operation from 1950–1973. Nine of these wells, shown in Fig. 2, are about 80 m deep, and have screens set at a depth of 50–70 m. Pumping samples were collected once or twice a year until the wells were shut down. Alkalinity and pH of the samples were not measured in the field, so some minor errors in these parameters probably exist. Nevertheless, the alkalinity values are about the same as the measured alkalinity in other water samples of the area (Martínez et al. 1997, 1998). Previously, Bocanegra et al. (1993) had analyzed the available groundwater-quality data to evaluate water-quality variations over time. In the present study, only a small group of samples was used for geochemical modeling.

Geochemical data from the two types of wells along the "normal groundwater-flow path" (the original flow path from the water divide toward the sea) were used: that from eight deep supply well (about 80 m deep; wells W35, W30, W7, W12, W18, W13, W3, W17 in Fig. 1) operated by Obras Sanitarias, and that from six shallow domestic wells (depths 12–25 m; wells 6, 7, 8, 10, 14, and 21 in Fig. 1) collected by the authors and analyzed in the Obras Sanitarias laboratory. Physicochemical parameters (temperature, pH, and conductivity) of groundwater from the shallow wells were measured in the field, and the chemical analyses were performed within 48 h of sample collection.

The chemical composition of the groundwater in the three wells selected for the study of the hydrochemical processes during marine intrusion are shown in Table 1. The chemical analyses are of samples taken before salinization (1950 and earlier) and after the process had started in 1957; also included is the calcite-saturation index for each sample. Table 2 shows the chemical composition of the well samples used for analysis of the chemical processes in the normal-flow path, and also some physicochemical parameters and the calcite-saturation index.

The geochemical data were plotted on Piper diagrams (Piper 1944) and subjected to hydrogeochemical modeling. Inverse mass-balance models were performed using NETPATH (Plummer et al. 1991). PHREEQM (Nienhius et al. 1991) was used for hydrogeochemical and 1-D-transport modeling. Besides the hydrogeochemical and 1-D-transport capabilities of PHREEQM, this code is also capable of modeling cation-exchange reactions and includes exchange coefficients in its database.

The adsorption capacity of a solid surface is mainly related to its specific surface (Stumm and Morgan 1981;

Table 1 Hydrochemical composition, ionic ratios, and calcite-saturation index ($SI_{calcite}$) of seawater and groundwater from selected wells in Mar del Plata before and after salinization. Well locations in Fig. 1

Well no.	Year sampled	pH	HCO_3^- (mg/L)	Cl^- (mg/L)	SO_4^{2-} (mg/L)	Ca^{2+} (mg/L)	Mg^{2+} (mg/L)	Na^+ (mg/L)	Ca/Na (molar)	Mg/Na (molar)	$SI_{calcite}$
Seawater		8.2	142	19,000	2,700	410	1,350	10,890	0.022	0.117	0.649
W3	1948	7.7	514	135	43	30	14	292	0.059	0.045	0.207
	1957	7.8	603	143	64	30	15	234	0.073	0.061	0.365
W7	1950	7.6	454	290	48	43	22	326	0.076	0.064	0.192
	1957	7.6	382	1,400	74	162	79	750	0.125	0.099	0.192
W12	1950	7.8	521	118	27	24	12	283	0.049	0.040	0.226
	1957	7.7	415	1,030	45	175	86	504	0.199	0.161	0.752

 DOI 10.1007/s10040-002-0195-7

Table 2 Chemical composition and physicochemical properties of groundwater from shallow and deep wells in the "normal-flow" path, Mar del Plata. Well locations in Fig. 1. *S* Shallow domestic well; *D* deep water supply well; $SI_{calcite}$ calcite-saturation index

Sample no. and type	pH	Conductivity (µs/cm)	Residue on evaporation (105 °C mg/L)	HCO_3^- (mg/L)	NO_3^- (mg/L)	Cl^- (mg/L)	SO_4^{2-} (mg/L)	Ca^{2+} (mg/L)	Mg^{2+} (mg/L)	Na^+ (mg/L)	K^+ (mg/L)	F^- (mg/L)	$SI_{calcite}$
2 S	7.5	1,410	924	700.3	41	116	36	50	24	279	11	0.5	0.343
6 S	7.5	950	638	402.6	72	54	19	56	30	117	12	0.5	0.203
7 S	7.7	850	548	395.3	46	52	9	46	30	119	15	0.9	0.321
8 S	7.8	1,050	751	514.8	53	65	19	28	13	219	9	1.1	0.308
10 S	7.5	750	523	395.3	8	44	18	117	8	40	2	0.5	0.529
11 S	7.6	950	573	419.7	63	66	9	43	31	138	8	0.3	0.188
12 S	7.2	850	539	270.8	25	132	11	69	39	60	7	0.8	–0.176
14 S	7.7	880	553	422.1	38	60	9	42	22	144	9	0.5	0.296
21 S	7.7	980	683	436.8	127	48	19	74	45	75	15	0.4	0.530
26 D	8.0	950	637	500.2	18	76	16	22	9	225	11	0.8	0.370
27 D	8.0	900	621	497.8	18	64	9	10	7	238	9	1.3	0.040
31 D	7.9	900	608	406.0	13	68	11	11	5	245	6	1.5	–0.820
32 D	8.0	840	623	412.0	14	76	10	15	8	211	9	1.1	0.140
33 D	8.0	800	549	358.0	27	52	6	26	15	211	13	1.3	0.210

Table 3 Sorption-related features and cation-exchange-capacity values of sediments from selected wells in the water-divide area, Mar del Plata, calculated from Breeuwsma et al. (1986). Well locations shown in Fig. 1

[a] In mg C/g of soil

Well no.	Depth (m)	Sand (%)	Clay (%)	Organic C[a] (%)	Organic matter (%)	CEC (meq/100 g)
P3	6	39.85	60.15	0.328	0.482	43.25
P3	8	53.69	46.31	0.448	0.772	33.98
P3	11	57.29	42.71	0.288	0.431	30.91
P1	12	58.10	41.9	0.448	0.772	30.90
P4	4	56.34	43.66	0.455	0.784	32.15
P5	39	44.0	56.0	0.408	0.703	40.60

Appelo and Postma 1993). Particles with large specific surfaces correspond to grain sizes that are in the clay fraction and in the associated organic matter. Thus, the cation-exchange capacity (CEC) of a sediment is a function of the percentages of clay, organic matter, and hydroxide content of the sediment. The empirical expression of Breeuwsma et al. (1986) describes this relationship:

$$\mathrm{CEC}\left(\mathrm{meq/L}\right) = 0.7\,(\%\mathrm{clay}) + 3.5\,(\%\mathrm{C}) \qquad (3)$$

Six samples of sediment from depths as great as 39 m in the aquifer, obtained from wells P1, P3, P4, and P5 along the water divide in an area underlain principally by clay(Fig. 1), were analyzed for sand, clay, and organic matter; from these the CEC values were calculated using Eq. (3). The results are shown in Table 3.

Results

Cation-Exchange Capacity of the Mar del Plata Aquifer

The calculated CEC in the Mar del Plata aquifer ranges from 30–43 meq/100 g. The CEC of selected samples from four wells was also measured directly in the laboratory. These results, shown in Table 4, range from 20–40 meq/100 g. Thus, about 40 meq/100g is the maximum value of CEC of the aquifer. No other CEC measurements exist for this aquifer.

Table 4 Cation-exchange capacity values of sediments from selected wells in the water divide area, Mar del Plata, measured in the laboratory

Well no.	Depth (m)	Sediment description	CEC (meq/100 g)
P3	6	Sandy silt and silt	19.8
P4	8	Caliche	35.2
P5	4	Sandy silt and silt	39.5
P5	14	Clay and clayey silt	38.8
P5	24	Sandy silt and silt	37.6
P5	35	Sandy silt and silt	34.4

CEC values for different clay minerals, presented in Stumm and Morgan (1981), Drever (1982), and Appelo and Postma (1993), are about 80–120 meq/100 g for smectite, 10–50 meq/100 g for illite, 100–200 meq/100 g for vermiculite, and <40 meq/100 g for chlorite. Reported CEC values for mixed sediments (Drever 1982) are 76 meq/100 g for the Ameca River (Mexico) sediments, 20–30 meq/100 g for the Aquia aquifer in Maryland (USA; Chapelle 1983), 14–17 meq/100 g for the Llobregat aquitard (Spain; Manzano et al. 1993). The values for the Mar del Plata aquifer, which is not a pure clay sediment, of 20–40 meq/100 g, are similar to those reported for mixed sediments.

 DOI 10.1007/s10040-002-0195-7

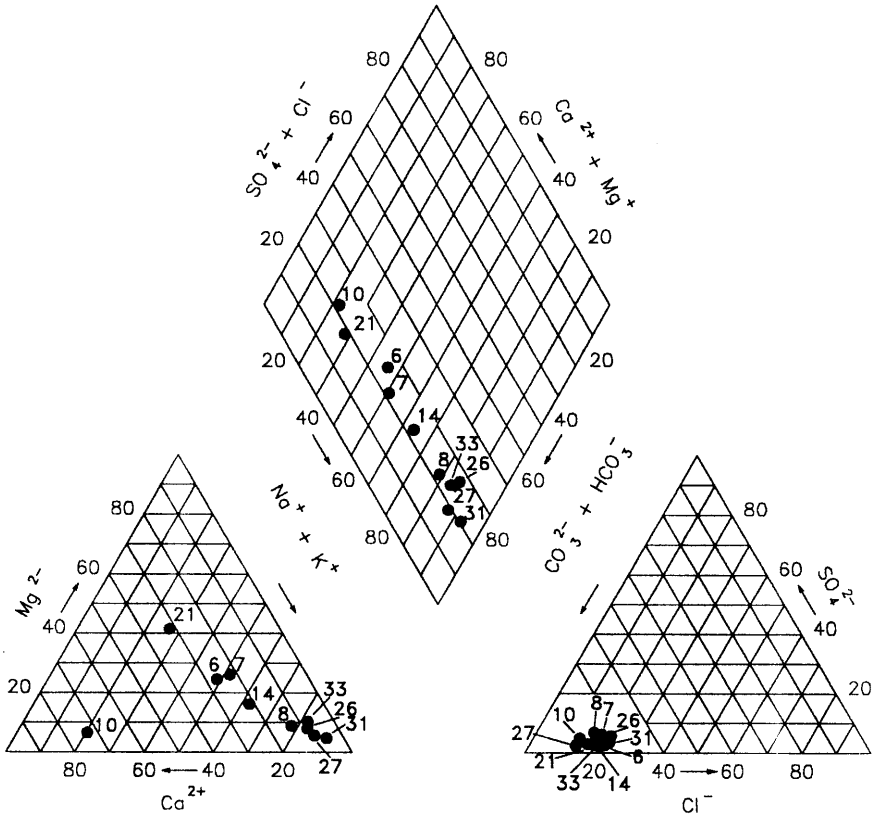

Fig. 5 Piper diagram showing the ionic composition of groundwater from selected wells in the watershed area (wells 10, 14, 21), transition and discharge areas (wells 6, 7, 8), and from deep supply wells (wells 26, 27, 31, 33), Mar del Plata. Data from Table 2. Well locations shown in Fig. 1

Table 5 Major-ion concentrations (mmol/L) in groundwater from selected wells in the normal flow path used in mass-balance modeling. Well locations shown in Fig. 1

Major element	Well no.			
	10	6	7	31
C total	6.913	7.049	6.737	6.814
S total	0.187	0.198	0.094	0.115
Cl^-	1.242	1.524	1.468	1.919
Ca^{2+}	2.921	1.398	1.148	0.275
Mg^{2+}	0.329	1.235	1.235	0.206
Na^+	1.741	5.093	5.180	10.665

The CEC values expressed in meq/100 g soil were recalculated to concentration units (meq/L pore water) using the formula (Appelo and Postma 1993):

$$\mathrm{CEC}\left(\mathrm{meq/L}\right) = \mathrm{CEC}\left(\mathrm{mg/100g}\right) \times 10 \times \rho_b/\varepsilon \qquad (4)$$

where ρ_b is the specific weight and ε is the porosity of the sediment. The value for the specific weight of 2.1 g/cm^3 is that for similar sediments in the area (Batallanez 1972). The measured porosity value of 0.30 for the aquifer is reported above. Differences in assumptions with respect to the specific weight do not have a high impact on the final result, but differences in the selected porosity value can result in important differences in the calculated CEC.

From Eq. (4), a CEC of about 2,400 meq/L is obtained for the Mar del Plata aquifer. This is high compared with the total content of cations in the solution, which ranges from 20–30 meq/L (expressed in mmol/L, Tables 5 and 6), so it is reasonable to assume that the availability of exchangeable surfaces is not restricted. However, over the long term, as large volumes of pore water move through the aquifer, the amount of cations transported in solution will exceed the exchange capacity of the aquifer.

Hydrogeochemical Inverse Modeling

Two scenarios were considered in analyzing the hydrogeochemistry and cation-exchange process in the Mar del Plata aquifer: the chemistry in the normal-flow path, and that in the marine-intrusion area, where the flow direction is reversed because of water-level decline below sea level.

Normal flow

The chemical distribution of selected water samples is plotted in the Piper (1944) diagram shown in Fig. 5. The samples represent the groundwater in the watershed area, the surface-discharge area (plains area in Fig. 1), and from deep in the aquifer.

The changes in ionic composition of the groundwater along the analyzed flow path in the aquifer are essentially the same. The sample from shallow wells in the watershed area is mainly the Ca-HCO_3 type, and the TDS content is 500–800 mg/L. These conditions suggest rapid in-

 DOI 10.1007/s10040-002-0195-7

Table 6 Major-ion concentrations (mmol/L) in seawater and in groundwater from selected wells, Mar del Plata, used in mass-balance modeling of seawater intrusion, using NETPATH. Well locations shown in Fig. 1

Major ions	Seawater	Well no. and sample year					
		W7		W12		W3	
		1950	1957	1950	1957	1948	1957
C	2.276	8.161	6.514	9.469	7.113	9.426	9.426
S	29.381	0.523	0.773	0.303	0.467	0.484	0.656
Cl^-	560.213	8.561	36.632	3.596	29.545	4.114	4.443
Ca^{2+}	10.498	1.028	4.076	0.555	4.313	0.694	0.645
Mg^{2+}	56.984	0.867	3.257	0.458	3.495	0.534	0.607
Na^+	486.108	13.583	32.695	11.419	21.657	11.783	12.321

Table 7 Results of mass-balance modeling of chemical processes in groundwater from selected wells, Mar del Plata, using NETPATH. Data from Table 2. Well locations are shown in Fig. 1. Processes refer to: *a* dissolution (positive sign) or precipitation (negative sign) of calcite; *b* dissolution (positive sign) or outgassing (negative sign) of CO_2 in an open system; *c* gypsum dissolution; *d* NaCl dissolution; *e* Ca/Na exchange, positive sign indicates the Ca^{2+} adsorption and the release of Na^+; molar ratio of 1:2; *f* Mg/Na exchange, positive sign indicates the Mg^{2+} adsorption and the release of Na^+; molar ratio of 1:2; *g* iron-sulfide precipitation

Well no.		Type of system	Process						
Initial[1]	Final[2]		a	b	c	d	e	f	g
10	31	Open	1.353	–1.452	–	0.677	3.999	0.123	–0.073
10	31	Closed	–0.991	–	1.452	0.677	3.999	0.123	–1.525
10	7	Open	0.833	–1.008	–0.094[3]	0.226	2.605	–0.905	–
10	6	Open	0.907	–0.771	0.010	0.282	2.440	–0.905	–
10	6	Closed	0.136	–	0.781	0.282	2.440	–0.905	–0.771

[1] *Initial* Groundwater samples from well recharge area
[2] *Final* Groundwater samples from wells in normal flow path
[3] Constraint ignored

filtration into the aquifer in which calcite equilibrium is the dominant process controlling water composition. The sample from shallow wells in the transition area (Fig. 3) is generally the Na–Ca-HCO_3 type, and the TDS content ranges from 600–1,000 mg/L. The water from deep wells is Na-HCO_3 type and has a TDS content of more than 1,000 mg/L.

Of the original sample set (Table 2), four samples from wells 10, 6, 7, and 31 were selected for use in the inverse modeling of the hydrogeochemical processes in the aquifer using the code NETPATH (Plummer et al. 1991). Well 10 (Fig. 1) was sampled because it is closest to the quartzite outcrops on the groundwater divide, so the flow path of the recharge is minimal and the water sample should closely resemble the recharge water. Well 7 is a shallow well in the same flow line as well 10, but about 1,000 m downgradient. Well 6, near the El Cardalito Creek, is in a local discharge area. The water chemistry of well 31 is representative of all the deep wells. Table 5 shows the molar concentration of the major ions in the groundwater from these wells. The following processes, shown in Table 7, were involved in the inverse modeling: (1) calcite equilibrium, (2) dissolution or outgassing of CO_2 in an open system, (3) gypsum dissolution (its precipitation is not possible according to the saturation state of the solutions), (4) NaCl dissolution, (5) Ca/Na exchange, (6) Mg/Na exchange, and (7) iron-sulfide precipitation. These particular processes were selected with regard to the mineralogy of the aquifer and the saturation state of the included minerals. Dissolution of NaCl was included to explain the chloride increase along the groundwater flow path. Halite was not observed in the aquifer, but, given the arid environment during the sediment deposition in the late Pleistocene, it is plausible to assume the presence of some chloride salts.

The saturation index (SI) of calcite in the normal-flow condition (–0.8 and 0.53; Table 2) indicates that the system is in equilibrium or slightly supersaturated; some samples exceed the 0–0.3 range considered normal for fresh waters. Calcite oversaturation could take place as a consequence of kinetic effects during dedolomitization and/or simultaneous gypsum dissolution (Plummer et al. 1990). In the present case, gypsum dissolution could contribute some to calcite oversaturation, but the higher SI values could be a result of sampling or analytical errors. A delay in making the alkalinity measurement could allow some CO_2 ingassing or outgassing, which would affect the analytical results.

Several available models can mimic the changes in composition from the water composition of well 10, located in the recharge area and considered to have the initial composition, to the water composition of the wells in the transition area, wells 6 and 7 and the deep well 31, are considered the final composition. The mass-balance modeling using NETPATH provides as many as three possible models that use different imposed constraints and phases. In each case, one of the resulting models

 DOI 10.1007/s10040-002-0195-7

Table 8 Results of mass-balance modeling of seawater/fresh-water mixing, Mar del Plata. Data from Table 7. Well locations are shown in Fig. 1. Processes refer to: *a* percentage of seawater calculated using chloride contents; *b* dissolution (positive sign) or precipitation (negative sign) of calcite; *c* dissolution (positive sign) or outgassing (negative sign) of CO_2 open system; *d* oxidation of organic matter (CH_2O) in redox process; *e* Ca/Na exchange, positive sign indicates the Ca^{2+} adsorption and the release of Na^+; molar ratio of 1:2; *f* Mg/Na exchange, positive sign indicates the Mg^{2+} adsorption and the release of Na^+;molar ratio of 1:2; *g* iron-sulfide precipitation

Well number (year sampled)			Process						
	Initial[1]	Final[2]	%	(mmol/L)					
			a	b	c	d	e	f	g
Seawater	W7 (‘50)	W7 (‘57)	5.63	–2.007	–	0.692	–4.522	0.771	–0.687
Seawater	W12 (‘50)	W12 (‘57)	4.66	–2.250	0.229	–	–5.544	–0.401	–0.591
Seawater	W3 ('48)	W3 ('57)	0.03	–0.111	–	–	–0.058	–0.196	0.306[3]

[1] *Initial* Groundwater samples collected from wells in 1948 and 1950

[2] *Final* Groundwater samples collected from wells in 1957

[3] Gypsum dissolution

does not include calcite equilibrium, which enhances the gypsum-dissolution processes and iron-sulfide precipitation. The models that include calcite equilibrium, however, are considered more likely to replicate aquifer conditions because of the abundance of calcite in the aquifer. Open-system models more closely simulate the observed chemical changes, including calcite dissolution, cation exchange, and outgassing of CO_2; moreover, some gypsum dissolution is involved. In Table 7, the results of the five mass-balance models that were considered the more realistic are shown. Five other models, including those that do not involve calcite equilibrium, were discarded.

Seawater intrusion

From a hydrochemical point of view, seawater intrusion is a mixing problem and the NETPATH code is a useful tool for analyzing it. To perform inverse modeling with NETPATH, a transect consisting of three wells, W7, W12, and W3 (Fig. 1), in a row roughly perpendicular to the coast, was selected. The chemical analyses, shown in Table 1, are of water samples collected from the wells in 1950, before seawater intrusion was verified, and samples collected in 1957 and 1958, after the salinization problem was detected.

NETPATH solves mass-balance models by applying the rule of phases; each major ion or chemical specie is considered a phase. When mixing is solved, it is considered to be an additional phase, and one less phase is needed to produce a complete model. The ion that is not included in any of the phases is used to calculate the mixing proportion according the formula:

$$C_f = p_1.C_1 + p_2.C_2 \quad (5)$$

where C_f is the concentration of the chemical species in the final composition, C_1 and C_2 are the concentrations in the initial solutions 1 and 2, respectively, and p_1 and p_2 are the mixing proportions of seawater and groundwater in the last collected samples.

A conservative ion, which does not participate in any reaction, must be used to establish the mixing proportions: chloride was chosen as the most convenient ion for this study. Bocanegra et al. (1993) obtained the mixed proportions of seawater (p_1) and groundwater (p_2) in evaluating the extent of salinization of the Mar del Plata aquifer by using only the chloride contents in the mass-balance calculations. The conservative composition is that resulting from the simple addition of the initial concentration of each ion C_1 and C_2 multiplied by the same mixing proportion, p_1 and p_2, obtained for chloride.

Comparing the major ionic composition of the last water sample from well W7, with the calculated conservative composition reported by Bocanegra et al. (1993), the following differences were obtained (in meq/L): Na^+ –29.5, Mg^{2+} –0.71, Ca^{2+} 17.4, HCO_3^- –2.49, SO_4^{2-} –6.14, and Cl^- 0.00. These differences can only be explained by the occurrence of various chemical reactions during the mixing process.

The chemical reactions included in the model depicting mixing are the same as those used in the normal-flow path modeling, plus the common reactions in freshwater/seawater mixing. Included in the models are the mixing of seawater and freshwater in the selected wells before salinization (1950), and the final composition of the groundwater in each well after salinization (1957 or 1958, Table 6). The results, shown in Table 8, indicate the proportion of seawater in the mixing ranges from 5.63% in well W7, the closest to the seaside, to 0.03% in well W3, the farthest away. The transfer of mass caused by calcite precipitation, Ca/Na exchange, and iron-sulfide precipitation is similar for wells W7 and W12. Although only slightly farther from the sea than well W12, the mass transfer in well W3 is considerably less.

The chemical changes in groundwater composition in the wells as a result of seawater intrusion, plotted in the Piper diagram (Fig. 6), can be readily discerned visually. From a temporal point of view, the changes from 1950–1958 in the water composition of wells W7 and W12 appear to be significant, whereas the water composition of W3 is little changed. The cationic composition

 DOI 10.1007/s10040-002-0195-7

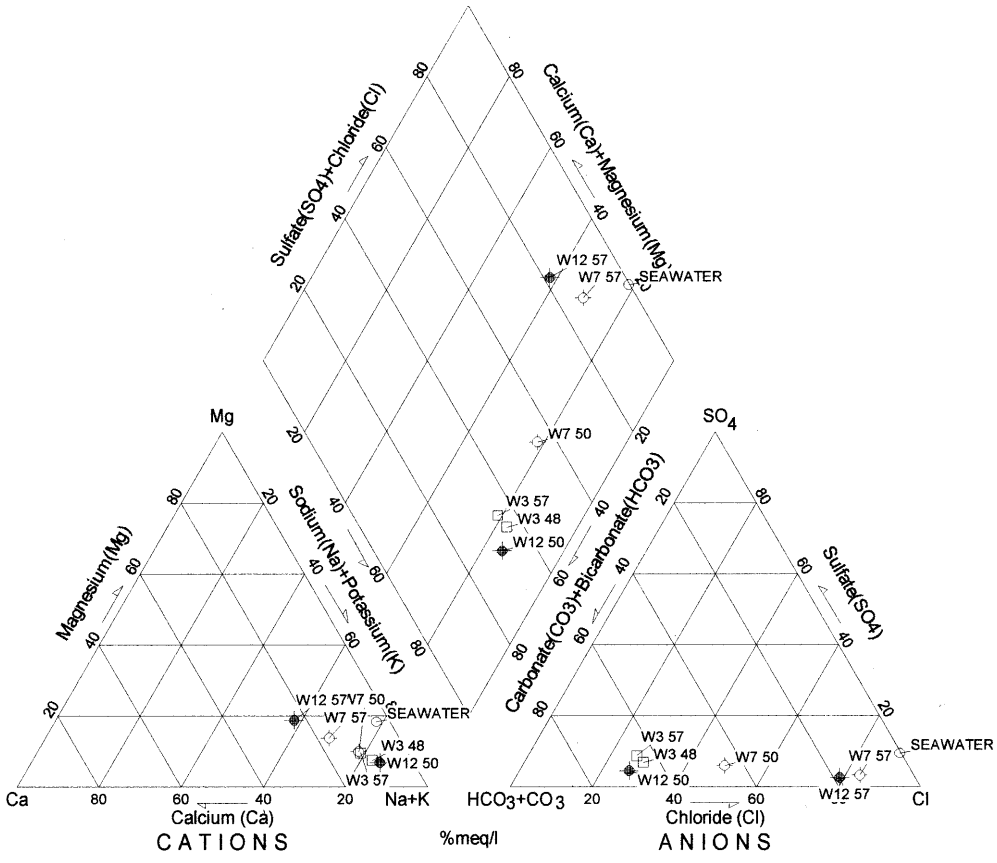

Fig. 6 Piper diagram showing the chemical composition of seawater and the hydrochemical changes in groundwater from selected wells along section *B–B´* because of seawater intrusion, Mar del Plata. Data from Table 1. Location of cross section in Fig. 2. Well numbers and sampling years are shown as W12 57

of water from wells W7 and W12 moves from about 80 to about 60%meq/L of sodium. The changes in the anionic composition of water in wells W7 and W12 are most noticeable, moving from bicarbonate waters not exceeding 50%meq/L of chloride, to chloride waters of more than 80%meq/L of chloride.

From a spatial point of view, no important chemical differences existed between the three wells before the marine intrusion, especially in the anionic composition. In the cationic composition, a little difference can be observed in well W3, which has a calcium content higher than that in wells W7 and W12, as explained earlier in the discussion of the normal flow evolution. The spatial distribution in 1957, after the marine intrusion, shows that water in the wells nearest the coast, W7 and W12, shifted to a sodium chloride composition, whereas water in well W3 remained a sodium bicarbonate water type.

The modeled results, shown in Table 8, exemplify both trends. In the temporal trend, water in wells W7 and W12 increased in chloride content because of seawater mixing, and in calcium composition because of cation exchange. Magnesium content decreased in well W7 and increased in well W12. From a spatial point of view, only the condition of the water in 1957 must be examined because, in 1950, the wells were in a normal-flow condition. The analyses (Table 8) show a decrease in the proportion of seawater in the wells in the inland direction from the coast, as would be expected.

Hydrogeochemical 1-D Transport Model

Using the PHREEQM code, a flow tube 1,500 m long was modeled to simulate piston flow in the transect between wells W7 and W12 at the beginning of the seawater intrusion process. The results of the inverse-geochemical modeling (Table 8) were used to select the processes to be included in the reactive-transport modeling. The flow-tube was divided into 30 cells, each 50 m long and each had their hydraulic parameters determined by Bocanegra et al. (1995; dispersivity 200 m, velocity 0.5 m/day, porosity 0.3), and the previously-determined mean cation-exchange capacity value (34.2 meq/100 g). The flow tube was initially filled with a chemical solution corresponding to the water in 1950 from the unsalinized aquifer at well 7 (Tables 1 and 6). Seawater was then allowed to enter in six increments from the "upper" end of the tube until the solution reached the same mixing characteristics as in well W7 in 1957. With each increment, a volume of seawater entered equal to the pore volume of a single cell, and each was called a step. With each step, the solution in each cell moved down and reacted, exchanged, and mixed with the next cell. The number of steps divided by the number of cells gives the number of pore volumes that flowed through the column.

Throughout the modeling, calcite equilibrium was maintained and the exchange reactions (Ca\Na, Mg\Na) were allowed to progress. The resulting compositions of

 DOI 10.1007/s10040-002-0195-7

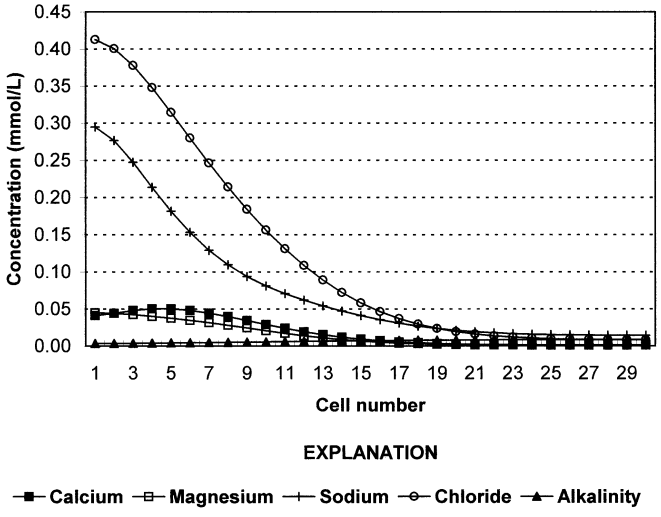

Fig. 7 Final major-ion composition in each cell of a flow tube initially containing unsalinized water of the composition of well W7 (1950) after introduction of seawater in six steps. Data from Table 1

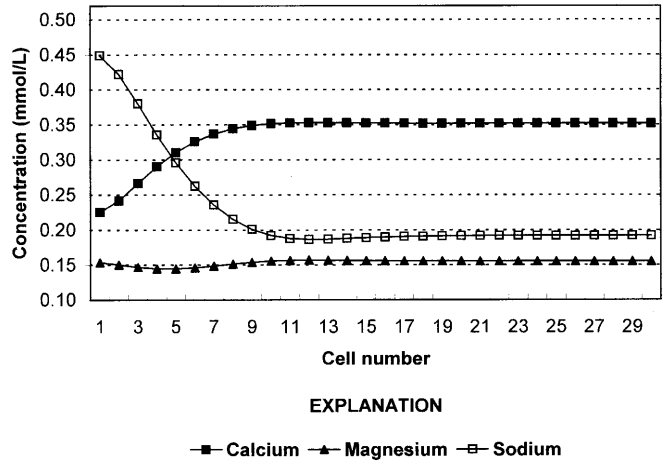

Fig. 8 Concentration of cations adsorbed on the exchange surfaces in each cell of the modeled flow tube after six steps of water mixing. Quality of the initial filling solution corresponds to that in the unsalinized aquifer (composition of well W7 in 1950) and seawater is entering by cell 1

the solution in each cell are shown in Fig. 7. The composition of the solution in each cell is not just from the mixing of seawater and fresh water, but also from cation-exchange and equilibrium processes. The increase in calcium content from cells 1–6 reveals the importance of the exchange processes. The exchange reactions are:

$$2Na^{+} + Ca{-}X_2 \Leftrightarrow 2Na{-}X + Ca^{2+} \quad (6)$$

$$2Na^{+} + Mg{-}X_2 \Leftrightarrow 2Na{-}X + Mg^{2+} \quad (7)$$

where X indicates the soil exchanger. The constants used for the reactions are calculated by PHREEQM using the equivalent fraction of exchangeable cations (Appelo and Postma 1993). Figure 8 shows the amounts of calcium, magnesium, and sodium attached to the exchanger surface in each cell at the end of the six steps. From inland (cell 30) to the coast (cell 1), from fresh water to increasingly saline water, the adsorbed sodium concentration increases, and, conversely, calcium is released, reducing its adsorbed concentration. Small amounts of magnesium were also released in cells 1–6. Magnesium was adsorbed in the cells that represent the more continental areas.

The composition of the groundwater from W7 (Table 6), the well closest to the coast, corresponds to the composition of the solution in cell 18 because this cell represents the equivalent distance from the coast. This cell is nearly the last one that clearly shows the effects of seawater mixing, and, therefore, was used to calibrate the model. A Schoeller diagram, illustrating the fit between the W7 water composition in 1957 and the cell 18 water composition in the model, is shown in Fig. 9.

Discussion

Analysis of the chemical changes along flow paths shows a variation in the cation composition, both in the normal-flow direction (Fig. 5) and along the seawater intrusion path (Fig. 6). Cation exchange is the most feasible explanation of the observed changes, but alternative hypotheses might be considered, mainly carbonate-equilibrium control of the alkaline-earth elements and/or a proportional sodium increase because of the high solubility of sodic salts. However, these alternatives would not be applicable in this marine-intrusion case because a sodium deficit and calcium excess cannot be explained on the basis of the solubility of the salts of these ions.

The results of inverse modeling obtained from the normal-case flow indicate that calcium/sodium exchange (with calcium uptake and sodium release) and calcite equilibrium are the two dominant geochemical processes controlling the groundwater composition. $Na^{+}\backslash Mg^{2+}$ exchange is probably a subordinate process. The observed order of affinity in water contacting the aquifer matrix is $Ca^{2+}>Mg^{2+}>Na^{+}$.

The strong increase in chloride in the groundwater from seawater intrusion is explained by the mixing of the waters: the seawater has about 19 g/L of Cl^{-}. In the case of marine intrusion, the exchange process is reversed. Sodium is removed from solution and calcium is released. Magnesium exchange is a secondary process. The cation replacement order during seawater intrusion is $Na^{+}>Mg^{2+}>Ca^{2+}$. Magnesium is released in the first steps of the process, but is later adsorbed. This process is shown in the 1-D transport model (Fig. 8). Reversal exchange of cations occurs when the adsorbed concentrations of sodium and calcium are equal. This fact is related to the $Ca^{2+}\backslash Mg^{2+}$ exchange, which is implicitly modeled.

The direction of a reaction of this type is:

$$Na^{+} + 1/2M{-}X_2 \Leftrightarrow Na{-}X + 1/2M^{2+} \quad (8)$$

 DOI 10.1007/s10040-002-0195-7

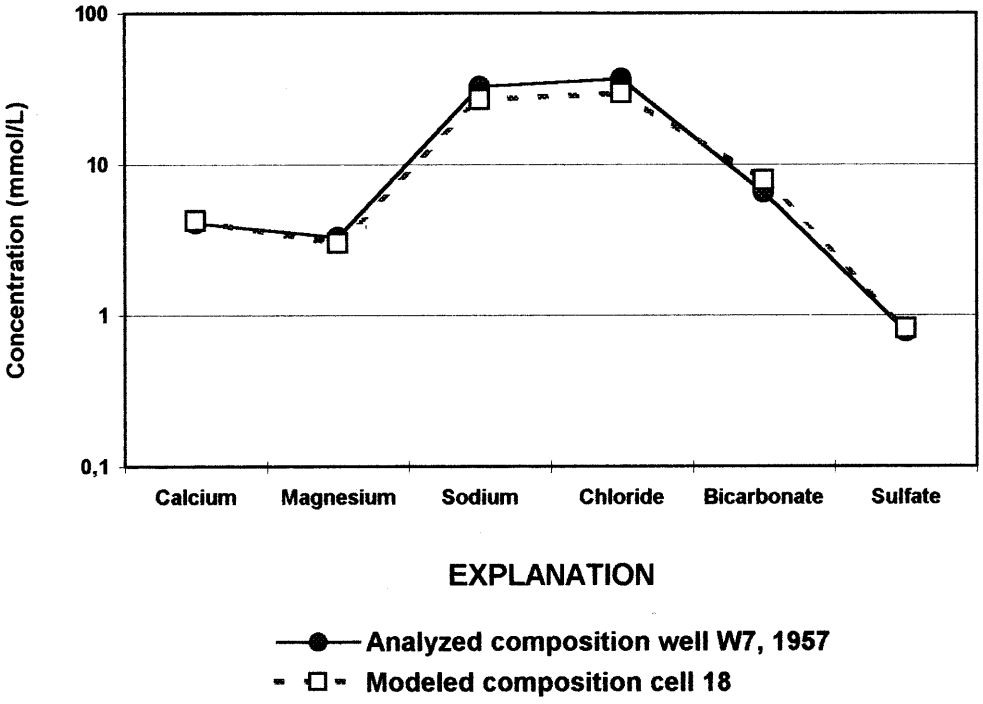

Fig. 9 Schoeller diagram comparing composition of groundwater in well W7 in 1957 with of solution in cell 18. Position of cell 18 corresponds to the distance of well W7 from the seacoast. Data from Table 2. Well locations shown in Fig. 1

where *M* represents a divalent cation, controlled by an equilibrium coefficient

$$K_{Na\backslash M} = [Na{-}X]\left[M^{2+}\right]^{0.5} \Big/ \left[Na^{+}\right][M{-}X_2]^{0.5} \qquad (9)$$

The equilibrium coefficient ($K_{Na\backslash M}$) depends on the type of exchanger (*X*) in the aquifer and also on the water composition. Equation (9) indicates the importance of the ion ratios in determining the sense of the exchange reaction. The molar-ion ratios for seawater are Ca/Na=0.022 and Mg/Na=0.12 (Table 1), whereas for groundwater in equilibrium with the aquifer matrix the ratios for Ca/Na are 0.049–0.076 and for Mg/Na they are 0.040–0.064. When these waters mix, the ionic ratios move away from equilibrium with the aquifer matrix. The equilibrium then tends to be restored by calcium release and sodium uptake. The greater selectivity for calcium rather than sodium leads to an initial magnesium release and calcium uptake in the Ca\Mg exchange, until the sodium and calcium concentrations become equal and this, in turn, leads to magnesium adsorption and sodium release.

Calcite equilibrium controls calcium concentrations in solution throughout the aquifer. The higher saturation index (SI) values are in samples from shallow wells in the water divide area (Fig. 1), and the lower values are in deep-well samples (Table 2). This relation is probably related to the adsorption of calcium along the flow path, which decreases the ionic-activity product (IAP). Calcite dissolution is greater in shallow groundwater as a result of the higher partial pressure of carbon dioxide (P_{CO2}) (log P_{CO2} –1.69) caused by respiration by the roots of plants. The seawater-fresh-water mixing produces an increase in SI values with respect to calcite (Table 1), and this leads to its potential for precipitation.

No significant changes were observed in the anion composition of the groundwater along the normal-flow path; bicarbonate waters prevail because of the unconfined nature of the aquifer and the important role of calcite equilibrium. Differences in sulfate concentration are not very important, but there is a general decline in sulfate concentration downgradient. Gypsum precipitation and iron-sulfide formation could influence this process. Iron-sulfide formation may be the dominant process controlling the decrease in sulfur concentrations in the seawater/fresh-water mixing area, where gypsum precipitation cannot occur because the solution is undersaturated with respect to gypsum. This process is described by Nadler et al. (1980) as occurring in many marine intrusion areas.

Conclusions

The most important geochemical processes controlling groundwater composition in the Mar del Plata aquifer are cation exchange and calcite equilibrium. Some iron-sulfide precipitation occurs, especially in the seawater/fresh-water mixing zone.

The replacement order of cations during cation exchange varies according to the particular location of the water in the aquifer relative to the recharge area and the interface with seawater. As groundwater flows from recharge to discharge areas, the cation-replacement order for cation exchange is $Ca^{2+}>Mg^{2+}>Na^{+}$. When the flow direction is reversed and seawater intrusion occurs, the replacement order during cation exchanges is also re-

 DOI 10.1007/s10040-002-0195-7

versed and becomes $Na^{+}>Mg^{2+}>Ca^{2+}$. Early in the salinization process, calcium is adsorbed and sodium and magnesium are released. When the adsorbed concentrations of calcium and sodium become equal, magnesium then becomes adsorbed. The shallow-groundwater zone in the aquifer is oversaturated in calcite, but in the deep zone of the aquifer calcite reaches equilibrium (SI=0) as a result of calcite precipitation and calcium adsorption in the flow path. Mixing with seawater produces an SI increase that leads to calcite precipitation.

The study also shows that the different zones of groundwater flow in the Mar del Plata aquifer can be characterized by various hydrogeochemical features. The relationship between flow zone and hydrochemical environment should be considered when specific analyses of solute transport (i.e., contamination studies) are performed. Moreover, the different affinity of the solid phase for mono or divalent cations in relation to the seawater-mixture proportion is an aspect that should be considered in many geochemical problems.

Acknowledgements The National University of Mar del Plata supported this research project. The authors are grateful to cartographers Virginia Bernasconi and Marcelo Farenga for the figures, and to Prof. Ma. Cecilia Serafini for contributing to the English version of the text. The comments and suggestions of the reviewers have contributed significantly to the improvement of the manuscript.

References

Appelo CAJ (1993). Analytical and numerical calculations of chromatographic patterns in aquifers. Proceedings of the XII Salt Water Intrusion meeting, Barcelona, Spain, CIMNE-UPC edn, pp 193–206

Appelo CAJ, Postma D (1993) Geochemistry, groundwater, and pollution. Balkema, Rotterdam, 536 pp

Back W, Herman JS (1991) Geochemical consequences of saltwater intrusion into carbonate aquifers. XXIII IAH Congress, Canary Islands, Spain, Proceedings I, pp 35–38

Back W, Hanshaw BB, Pyle TE, Plummer LN, Weidie AE (1979) Geochemical significance of groundwater discharge and carbonate solution to the formation of Caleta Xel Ha, Quintana Roo, México. Water Resour Res 15(6):1521–1535

Banks HO, Richter RC, Harder J (1957) Seawater intrusion in California. Am Water Works Assoc J 49:71–88

Batallanez EE (1972) Capacidad de almacenaje de humedad de cuatro suelos del sudeste de la provincia a de Buenos Aires [Water retention capacity of four soils of the southeast of the Province of Buenos Aires]. Trabajo de Graduación, Universidad católica de Mar del Plata, Facultad de Agronomía, 56 pp

Beekman HE (1991) Ion chromatography of fresh and salt water intrusions. PhD Thesis, Free University, Amsterdam, The Netherlands, 198 pp

Bocanegra EM (1993) Modelación hidrogeoquímica de los procesos de salinización del acuífero de Mar del Plata [Hydrogeochemical modeling of the process of salinization in Mar del Plata aquifer]. In: Bocanegra E, Rapaccini A (eds) Temas Actuales de la Hidrología Subterránea, Publishing Service of the Universidad Nacional De Mar Del Plata, Mar Del Plata, pp 349–360

Bocanegra EM, Custodio E (1994) Utilización de acuíferos costeros para abastecimiento. Dos casos de estudio [The use of coastal aquifers for water supply. Two study cases: Mar del Plata (provincia de Buenos Aires, Argentina) and Barcelona (Cataluña, Spain)]. Ing Agua 1(4):49–78

Bocanegra EM, Benavente M, Cionchi JL (1995). Simulación numérica del proceso de transporte de cloruros en el acuífero de Mar del Plata [Mathematical simulation of chloride transport in Mar del Plata aquifer]. Ser Correlación Geol, UN Tucuman 11:25–32

Bocanegra EM, Martinez DE, Massone HE, Cionchi JL (1993) Exploitation effect and salt water intrusion in Mar del Plata aquifer, Argentina. Proceedings of the XII Salt Water Intrusion Meeting, Barcelona, Spain, CIMNE-UPC edn, pp 177–191

Bosch X, Custodio E (1993) Dissolution processes in the freshwater–saltwater mixing zone in the Cala Jostel area (Vandellós, Tarragona). Proceedings of the XII Salt Water Intrusion Meeting, Barcelona, CIMNE-UPC edn, pp 229–244

Breeuwsma A, Wösten JMH, Vleeshouwer JJ, Van Slobe AM, Bouma J (1986) Derivation of land qualities to assess environmental problems from soil surveys. Soil Sci Soc Am J 50:186–190

Carber RE (1971) Procedures in sedimentary petrology. Wiley-Interscience, Chichester, 647 pp

Chapelle FH (1983) Groundwater geochemistry and calcite cementation of the Aquia aquifer in southern Maryland. Water Resour Res 19(2):545–558

Custodio E (1987) Sea-water intrusion in the Llobregat Delta, near Barcelona (Catalonia, Spain). Groundwater problems in coastal areas. Studies and reports in hydrology, no 45. UNESCO, Paris, pp 436–463

Custodio E, Llamas MR (1976) Hidrología Subterránea [Underground hydrology], vol 1–2. Ediciones Omega, Barcelona, 2350 pp

Dalla Salda L, Iñíguez M (1979) La Tinta, Precámbrico y Paleozoico de Buenos Aires [La Tinta, Precambrian and Paleozoic of Buenos Aires]. VII Congr Geol Argentino Actas I:539–550

Drever JI (1982) The geochemistry of natural waters. Prentice Hall, Englewood Cliffs, New Jersey, USA, 387 pp

El-Baruni SS (1995) Deterioration of quality of groundwater from Suani wellfield, Tripoli, Libya. Hydrogeol J 3(2):58–64

Giménez E, Morell I, Fidelibus MD (1995) Importancia de los procesos de intercambio iónico en la caracterización de la intrusión marina en el acuífero de Oropesa (Castellón-España) [The importance of the ionic-exchange processes in the characterization of seawater intrusion in the Oropesa aquifer (Castellón, Spain)]. Ser Correlación Geol, UN Tucuman 11:183–182

Groeber P (1954) Geología e hidrología de Mar del Plata en relación con el problema del suministro de agua potable a la población urbana [The geology and hydrogeology of Mar del Plata: their relation to the problem of fresh-water supply]. Rev Mus Cs Naturales Trad Mar del Plata 1:5–24

Kohout FA (1960) Flow pattern of fresh water and salt water in the Biscayne aquifer of southeastern Florida. J Geophys Res 65:2133–2141

Manzano M, Custodio E, Carrera J (1993) Fresh and salt water in the Llobregat Delta aquitard: application of the ion chromatography theory to the field data. Proc XII Salt Water Intrusion meeting, Barcelona, CIMNE-UPC edn, pp 207–228

Martínez DE, Bocanegra EM (1998). Procesos de intercambio catiónico en el acuífero de Mar del Plata, Argentina [Cation-exchange processes in the aquifer of Mar del Plata, Argentina]. IV Congreso Latinoamericano de Hidrología Subterránea, Montevideo, Uruguay, Actas 3, pp 1385–1399

Martínez DE, Bocanegra EM, Cionchi JL (1995) Modelación hidrogeoquímica de procesos de mezcla. Su aplicación a dos casos de estudio en el acuífero de Mar del Plata [Hydrogeochemical modeling of mixing processes. Its application to two study cases in the aquifer of Mar del Plata]. Ser Correlación Geol, UN Tucuman 11:69–80

Martínez DE, Bocanegra EM, Costa JL (1997) Significado de la correlacion $pH/NO_3^{-}/Ca^{2+}/Mg^{2+}$ en aguas subterraneas del sudeste de la provincia de Buenos Aires [The meaning of the $pH/NO_3^{-}/Ca^{2+}/Mg^{2+}$ correlation in the groundwaters of the southeast of the Province of Buenos Aires]. I Congreso Nacional de Hidrogeología, Bahía Blanca, Actas, pp 193–210

 DOI 10.1007/s10040-002-0195-7

Martínez DE, Osterrieth M, Maggi J (1998). Equilibrio químico solución-fase mineral en el acuífero clástico de la cuenca superior del Arroyo Loberia, Partido de Gral. Pueyrredón [Chemical equilibrium of the solution-mineral phases in the detritic aquifer of the upper basin of Lobería Creek, Gral. Pueyrredón District]. VI Jornadas Geológicas Bonaerenes, Mar del Plata, 9 al 11 de diciembre, Actas 2, pp 23–32

Nadler A, Margaritz M, Mazor E (1980) Chemical reactions of seawater with rocks and freshwater: experimental and field observations on brackish waters in Israel. Geochim Cosmochim Acta 44:879–886

Nienhuis P, Appelo T, Willemsen G (1991) PHREEQM, PHREEQE in a mixing cell tube, user guide. Free University, Amsterdam, The Netherlands, 17 pp

Osterrieth M (1992) Pirita framboidal en secuencias sedimentarias costeras del Holoceno tardío en Mar Chiquita, Buenos Aires, Argentina [Framboidal pyrite in coastal sedimentary sequences of late Holocene age in Mar Chiquita]. IV Reunión Argentina de Sedimentología, Las Plata, Argentina, Actas 2, pp 73–80

Piper AM (1944) A graphic procedure in the geochemical interrelation of water analyses. Geophys Union Trans 25:914–923

Plummer LN, Busby JF, Lee RW, Hanshaw BB (1990) Geochemical modeling of the Madison aquifer in parts of Montana, Wyoming, and South Dakota. Water Resour Res 26(9):1981–2014

Plummer LN, Prestemon EC, Parkhurst DL(1991) An interactive code (NETPATH) for modeling NET geochemical reactions along a flow PATH. US Geol Surv Water Resour Invest 4078, 227 pp

Sala JM, Hernandez M, Gonzalez M, Kruse E, Rojo E (1980) Investigacion geohidrologica aplicada en el area de Mar del Plata [Applied hydrogeological research in the area of Mar del Plata]. Convenio OSN, Univ de La Plata 5(3), 65 pp

Sposito G (1984) The surface chemistry of soils. Oxford University Press, New York, 234 pp

Steinich B, Escolero O, Martin LE (1998) Salt water intrusion and nitrate contamination in the Valley of Hermosillo and El Sahuaral coastal aquifers, Sonora, Mexico. Hydrogeol J 6(4):518–526

Stumm W, Morgan JJ (1981) Aquatic chemistry. Wiley, Chichester, 780 pp

Stuyfzand PJ (1993) Behavior of major and trace constituents in fresh and salt water intrusion waters, in the western Netherlands. Proc. XII Salt Water Intrusion Meeting, pp 143–160

Stuyfzand PJ (1999) Patterns in groundwater chemistry resulting from groundwater flow. Hydrogeol J 7(1):15–27

Teruggi ME (1957) The nature and origin of Argentine loess. J Sediment Petrol 27(3):322–332

Teruggi ME, Kilmurray J (1980) Sierras Septentrionales de la Provincia de Buenos Aires [Northern mountain range of the province of Buenos Aires]. II Simp Geol Regional Arg, Acad Nac Cienc I:359–372

Thornthwaite C (1948) An approach toward a rational classification of climate. Geogr Rev 35(1):55–94

Walkey A, Black A (1965) Organic carbon. In: Black CA (ed) Methods of soil analysis. American Society of Agronomy, Madison, Wisconsin, USA, pp 1372–1374

Walraevens K, Boughriba M, De Breuck W (1993) Groundwater quality evolution in the Black-Sluice polder area around Assenede (Belgium). Proc XII Salt Water Intrusion meeting, Barcelona, CIMNE-UPC edn, pp 121–142

Wigley TM, Plummer LN (1976) Mixing of carbonate waters. Geochim Cosmochim Acta 40:989–995

 DOI 10.1007/s10040-002-0195-7